Colloids and Surfaces B: Biointerfaces 140 (2016) 176–184

Contents lists available at ScienceDirect

Colloids and Surfaces B: Biointerfaces

journal homepage: www.elsevier.com/locate/colsurfb

Poly(L-histidine) based copolymers: Effect of the chemically substituted L-histidine on the physio-chemical properties of the micelles and *in vivo* biodistribution

Xiaojun Zhang, Dawei Chen, Shuang Ba, Jing Chang, Jiaying Zhou, Haixia Zhao, Jia Zhu, Xiuli Zhao, Haiyang Hu, Mingxi Qiao*

School of Pharmacy, Shenyang Pharmaceutical University, P.O. Box 42, Wenhua Road 103, Shenyang, Liaoning Province 110016, PR China

ARTICLE INFO

Article history:
Received 6 July 2015
Received in revised form
21 November 2015
Accepted 18 December 2015
Available online 23 December 2015

Keywords:
pH-sensitive
Micelles
Doxorubicin
Chemical substitution
L-histidine

ABSTRACT

Even though the Poly(L-histidine) (PHis) based copolymers have been well studied, the effect of the chemically substituted L-histidine on the physio-chemical and biological properties of the micelles has never been elucidated to date. To address this issue, triblock copolymer of poly(ethylene glycol)-poly(D,L-lactide)-poly(2,4-dinitrophenol-L-histidine)(mPEG-b-PLA-b-DNP-PHis) with DNP group substituted to the saturated nitrogen of L-histidine were synthesized. The pH sensitive properties of the copolymer micelles were characterized using an acid-base titration method, fluorescene probe technique, DLS observation, *in vitro* drug release and cytotoxicity against MCF-7 cells under different pH conditions, respectively. The results suggest that mPEG-b-PLA-b-DNP-PHis copolymers showed similiar micellar stability for DOX loaded micelles, increased particle size, and similar pH responsive properties with mPEG-b-PLA-b-PHis copolymers. The subcellular distribution observation demonstrated that mPEG-b-PLA-b-DNP-PHis micelles showed a slightly compromised endo-lysosmal escape of doxorubicin as compared to mPEG-b-PLA-b-PHis micelles. The mPEG-b-PLA-b-DNP-PHis micelles showed higher cellular uptake by MCF-7 cells than mPEG-b-PLA-b-PHis micelles due to the different uptake pathways. Effect of DNP substitution on the *in vivo* distribution of the copolymer micelles was studied using non-invasive near-infrared fluorescence (NIRF) imaging with mPEG-b-PLA-b-PHis micelles as control. The results indicate that the mPEG-b-PLA-b-DNP-PHis micelles showed a reduced passive targeting to the tumor due to the larger particle size. These results suggest that saturated nitrogen of PHis may serve as a valuable site for chemical modification of the PHis based copolymers because of the little effect on the pH responsive properties. However, selection of the substitution group needs to be considered due to the possible increase of micellar particle size of the micelles, leading to compromised passive targeting.

1. Introduction

pH sensitive poly(L-histidine) (PHis)-based copolymer micelles have attracted great attention in the targeted delivery of anticancer drugs during the last decade due to the universally acidic tumor microenvironment [1–5]. PHis contains pendent imidazole groups that undergo hydrophobic to hydrophilic transition at acidic pH because of the protonation of the unsaturated nitrogens in the imidazole groups [6] (Fig. 1). The pH dependent amphoteric transition of PHis has been utilized in an attempt to trigger anticancer drug release in response to tumor extracellular pH (pH_e) or endosomal pH (pH_{endo}) [7,8]. However, amphiphilic copolymers composed of PHis block could not satisfy the requirement for pH_e or pH_{endo} triggered drug release. For example, the mPEG-PHis copolymer micelles demonstrated slightly higher triggering pH than pH_e due to the partially protonated PHis at pH 7.4, leading to less stable micelles at the pH [9,10]. Therefore, PHis based copolymers have been either mixed with other copolymers to form mixed micelles or chemically modified to precisely tune the triggering pH for the expecting accelerated drug release [11–15]. The triggering pH of the copolymer micelles could be shifted to a more appropriate value than unmodified PHis copolymers due to the hydrophobic modification.

The poly(L-histidine) peptides were usually synthesized by a classical ring-opening polymerization (ROP) of amino acid *N*-carboxy-anhydride (NACs) [16]. Dinitrophenol (DNP) was com-

* Corresponding author. Fax: +86 24 23986306.
E-mail address: qiaomingxi@163.com (M. Qiao).

http://dx.doi.org/10.1016/j.colsurfb.2015.12.032
0927-7765/

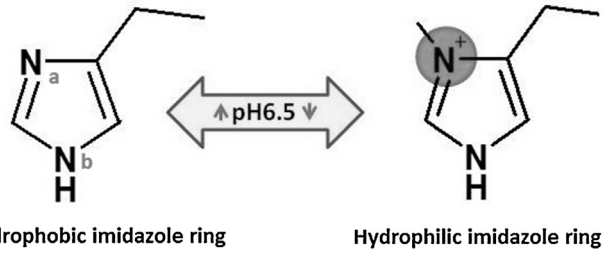

Fig. 1. The pH-dependent protonation of imidazole group of PHis. (a) Unsaturated N atom in the imidazole ring; (b) saturated N atom in the imidazole ring.

monly used as a protection group to the saturated nitrogen of *N*-carboxy-anhydride (NCA) monomers to avoid the side reaction with NCA or other activated amino acid derivatives [17]. In order to ensure a succesful synthesis, after ring-opening polymeration, the conjugated DNP groups were cut off by thiolysis to obtain poly(L-histidine) [18,19]. Because the unsaturated nitrogen of the imidazole ring in the PHis block accounted for the pH responsive properties, the removal of the protection groups from saturated nitrogen seems unnecessary for ensurance of the pH responsive properties. More importantly, the saturated nitrogen offers a valuable chemical modification site for improving the formation properties of the micelles. Despite the promise of the micelles in encapsulation hydrophobic drugs and tumor targeting delivery, drug delivery has been challenging due to the limited drug loading and *in vivo* stability. Recent studies in this aspect have demonstrated that properly chemical modification to the core-forming block was able to increase the hydrophobic interactions, hydrogen bonding interactions and electrostatic interactions with the payload as well as the core crystallinity and π–π stacking, leading to improved drug loading and *in vivo* stability. For example, hydrophobic modification to the core forming block of PEG-poly(trimethylene carbonate) (PTMC) with cholesteryl 2-(5-methl-2-oxo-1,3-dioxane-5-carboxyloyloxy) ethyl carbamate groups demonstrated to higher paclitaxel loading and improved kinetic stability [20]. Incorporating hydrogen-bond donors and acceptors into the polymer can also facilitate improved drug loading and stability, as indicated by the molecular dynamics simulation of cucurbitacin and polycaprolactone [21]. By introducing an opposite charge to the hydrophobic block, the electrostatic interactions of the hydrophobic block with siRNA within the core provided a sustained release profile and increased stability [22]. In addition, the saturated nitrogen of poly(L-histidine) could be also chemically modified to integrate a new function in order to engineer a poly(L-histidine) based multifunctional micelles.

Eventhough the poly(L-histidine) based micelles have been investigated by other research group, such as PLA-PEG-poly(L-histidine) by E.S. Lee et al. [1], PEG-poly(L-histidine)-PLA by R. Liu et al. [23], and PEG-PLA-Poly(L-histine) by our group [24], little researches have been conducted using chemically substituted poly(L-histidine). Moreover, the effect of chemically substituted poly(L-histidine) on the physio-chemical and biological properties of the poly(L-histidine) based micelles have not been elucidated to date. In this study, mPEG-b-PLA-b-DNP-PHis with DNP substituted to the saturated nitrogen of L-histidine was synthesized to investigate the effect of the substitution group on the formulation characteristics, pH responsive properties, cellular uptake and *in vivo* biodistribution of the copolymer based micelles. The significance of the paper is to indicate if the saturated nitrogen of poly(L-histidine) can be used as a modification site in order to improve the formulation properties of the micelle for drug delivery.

2. Experimental

2.1. Materials

Nα-CBZ-N^{im}-DNP-L-histidine was purchased from GL Biochem (Shanghai,China). Poly(ethylene glycol) methyl ether (mPEG, Mw: 2000 g/mol) was purchased from Sigma–Aldrich Co., D, L-lactide was purchased from GLACO (Beijing, China). Isopropylamine was purchased from Sinopharm Chemical Reagent Co. (Shanghai, China). *N*, *N*′-carbonyldiimidazole (CDI) was purchased from J&K Ltd. (Beijing, China). Doxorubicin (DOX) was purchased from Beijing HuaFeng United Technology Co., Ltd. (Beijing, China). Lysotracker Green was purchased from Beyotime Biotechnology Co,, Ltd, (Nantong,China). Hoechst 33258 and 3-(4,5-dimethyl-thiazol-2-yl)-2,5-diphenyl-tetrazolium bromide (MTT) were purchased from Sigma (St. Louis, MO, USA). The fluorescent compound, 1,1-dioctadecyl-3,3,3,3-tetramethylindotricarbocyanine iodide (DiR) was purchased from ATT bioquest, Inc. (Sunnyvale, USA). Purified deionized water was prepared by the Milli-Q plus system (Millipore Co., Billerica, MA, USA). Thionyl chloride ($SOCl_2$), dichloromethane (CH_2Cl_2), *N*, *N*-dimethylformamide (DMF), Dimethyl sulfoxide (DMSO), Tetrahydrofuran (THF), Acetonitrile (ACN) were purchased from Bodi Ltd. (Tianjin,China). All the other reagents and chemicals were of analytical or chromatographic grade and were purchased from Concord Technology (Tianjin, China).

The human breast cancer cell line MCF-7 was purchased from American Type Cell Culture (ATCC, Manassas, VA). Culture plates and dishes were purchased from Corning Inc. (New York, NY). MCF-7 cells were cultured in DMEM medium, supplemented with 10% fetal bovine serum (FBS), 100 IU/mL penicillin and 100 IU/mL streptomycin sulfate. All cells were cultured at 37 °C in a humidifier with 5% CO_2 atmosphere.

Female BALB/c nude mice (20 ± 2 g), supplied by Department of Experimental Animals, Shenyang Pharmaceutical University (Shenyang, China), were acclimated at 25 °C and 55% of humidity under natural light/dark conditions. All animal experiments were carried out in accordance with guidelines evaluated and approved by the ethics committee of Shenyang Pharmaceutical University.

2.2. Synthesis and characterization of copolymers

The mPEG-b-PLA-b-DNP-PHis copolymer were synthesized according to our previous study [24]. The details are shown in supplementary material. The molecular weights of the copolymers were determined by ^{1}H NMR and GPC, respectively.

2.3. Acid-base titration

The buffering capacities of mPEG-b-PLA-b-PHis and mPEG-b-PLA-b-DNP-PHis copolymers were measured by acid-base titration method [25]. The copolymer (30 mg) was dissolved in 10 mL of 0.01 M NaOH solution and the solution was adjusted to pH 11 with 1 M NaOH. The diluted copolymer solution was titrated by stepwise addition of 0.01 M HCl to obtain the titration profile. The buffering capacity is defined as the percentage of unsaturated nitrogen groups become protonated from pH 7.4 to pH 4.0, which can be calculated as follows [26,27]:

$$\text{Buffering capacity} = \frac{\Delta H^{+}_{\text{Copolymer}} - \Delta H^{+}_{NaCl}}{n} \times 100\%$$

wherein $\Delta H^{+}_{\text{Copolymer}}$ and ΔH^{+}_{NaCl} are the moles of H^+ required to adjust the pH of copolymer solution and 0.1 M NaCl from pH 7.4 to pH 4.0, respectively, and n is the total moles of unsaturated nitrogens in imidazole groups in the copolymer.

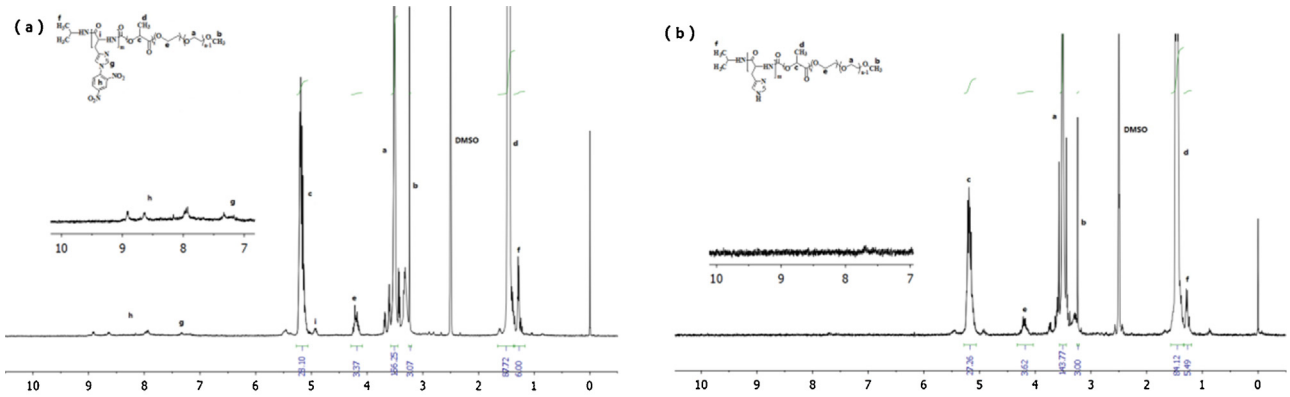

Fig. 2. The typical ^{1}H NMR spectra of PHis based copolymer (a) mPEG-b-PLA-b-DNP-PHis; (b) mPEG-b-PLA-b-PHis.

Table 1
Characterization of the PHis based triblock copolymers.

Copolymers	M_w[a](Da)	M_n[a](Da)	M_w/M_n[a]	M_w[b](Da)	Buffering capacity (pH 7.4–4.0) (%)	CMC (μg/mL)	Zeta potential (mV)
mPEG-b-PLA-b-PHis	3882	3512	1.105	4940	26.76	4.26	−17.5
mPEG-b-PLA-b-DNP-PHis	5361	4578	1.171	5114	19.26	3.65	−21.0
mPEG-b-PLA	3232	2971	1.088	3296	–	11.5	−2.5

The data of mPEG-b-PLA-b-PHis copolymer that have been published before were used again for comparision [24].
[a] Determined from GPC analysis.
[b] Calculated from ^{1}H-NMR spectrum.

2.4. Measurement of critical micelle concentration (CMC)

The critical micelle concentrations (CMC) of the copolymers were determined using a fluorescence spectrophotometer with pyrene as a probe. A stock solution of pyrene (6.0×10^{-6} M) was prepared in acetone and stored at 4 °C. The pyrene solution was dropped into various brown volumetric flasks and the solvent was evaporated under vacuum at 60 °C. A series of copolymer micelle solutions (0.5–100 μg/mL) were added to the flasks. All the volumetric flasks were stored in the dark place for 24 h to reach solubilization equilibrium prior to measurement. Fluorescence excitation spectra were measured using a Fluorescence Spectroscopy (Shimadzu RF-5301PC) with excitation and emission slit widths fixed at 2.5 and 5.0 nm, respectively. The change of the intensity ratio (I_{336}/I_{334}) of the pyrene as a function of log concentration was plotted from excitation spectra from 300 to 350 nm and at emission wavelength 397 nm. The CMC was determined from crossover point at low copolymer concentration from the plot.

The intensity ratios (I_{336}/I_{334}, higher ratios means a less polar environment) of the pyrene at different pH values (pH 8.5–4.5) were also measured to quantify the polarity around the pyrene molecules retained in the copolymer micelles [1].

2.5. In vitro *cytotoxicity*

The *in vitro* cytotoxicity of DOX-loaded micelles was assessed by a standard MTT assay [28,29]. The MCF-7 cells were seeded in 96-well plates at the density of 7000 cells per well. After overnight incubation, the DMEM medium was removed and replaced with fresh DMEM medium containing tested samples. The cells were incubated for 48 h, then 20 μL of MTT solution (5 mg/mL in PBS 7.4) was added to each well. After the cells were incubated for an additional 4 h at 37 °C, the medium was removed carefully. The received blue formazan crystals were dissolved in 150 μL of DMSO for each well, and the absorbance was measured in a Multifuctional microplate reader (Tecan, Austria) at the wavelength of 570 nm [30].

2.6. Preparation of DOX and DiR loaded copolymer micelles

The DOX base was obtained from doxorubicin hydrochloride in the presence of triethyl amine [24,31]. DOX-loaded micelles were prepared by thin-film rehydration method [32]. DOX and copolymers were co-dissolved in 10 mL of acetonitrile (ACN). The solvent was removed by rotary evaporation at 60 °C to obtain a thin film. Residual ACN remaining in the film was further evaporated overnight at room temperature under vacuum. The thin film was hydrated with 10 mL of PBS 7.4 for 30 min to obtain micellar solution. The micellar solution was filtered through a 0.45 μm film to remove the unincorporated DOX aggregates. The blank copolymer micelles prepared as described above without adding DOX. The DiR-loaded copolymer micelles were prepared by a same procedure except an addition of a 200 μL DiR ethanol (2.5 mg/mL) solution to the ACN solution containing copolymer.

The drug loading content (DL %) and encapsulation efficiency (EE %) were calculated by the following equations [33], respectively.

$$\mathrm{DL}(\%) = \frac{\mathrm{Weight\ \ ofdruginthemicelles}}{\mathrm{Weight\ \ ofdrug\ \ incorporatedmicelles}} \times 100$$

$$\mathrm{EE}(\%) = \frac{\mathrm{Weight\ \ of\ \ the\ \ druginmicelles}}{\mathrm{Weight\ \ of\ \ the\ \ feeding\ \ drug}} \times 100$$

2.7. Dynamic light scattering

Dynamic light scattering (DLS) was used to measure the mean hydrodynamic diameter and particle size distribution of the copolymer micelles ($n = 3$). All the measurements were carried out on a Zetasizer Nano ZS (Malvern, UK) at 25 °C after equilibration for 5 min. The micellar solutions were filtered through a 0.45 μm disposable membrane filter prior to measurement.

2.8. Transmission electron microscopy (TEM)

The morphology of the copolymer micelles was observed using a JEOL JEM-2100 electron microscope (Jeol Ltd., Tokyo, Japan) with an

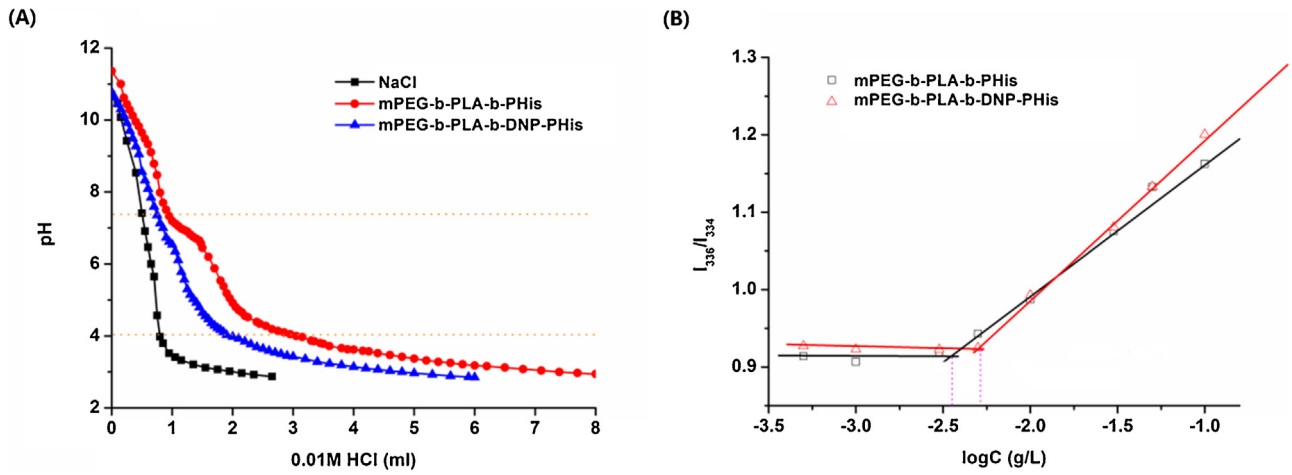

Fig. 3. Acid-base titration curves of the PHis based copolymers with NaCl as control (A); the fluorescence intensity ratio of I_{336}/I_{334} ratio from emission spectra *vs.* log concentration of copolymer (B). The data of mPEG-b-PLA-b-PHis copolymer that have been published before were used again for comparision [24].

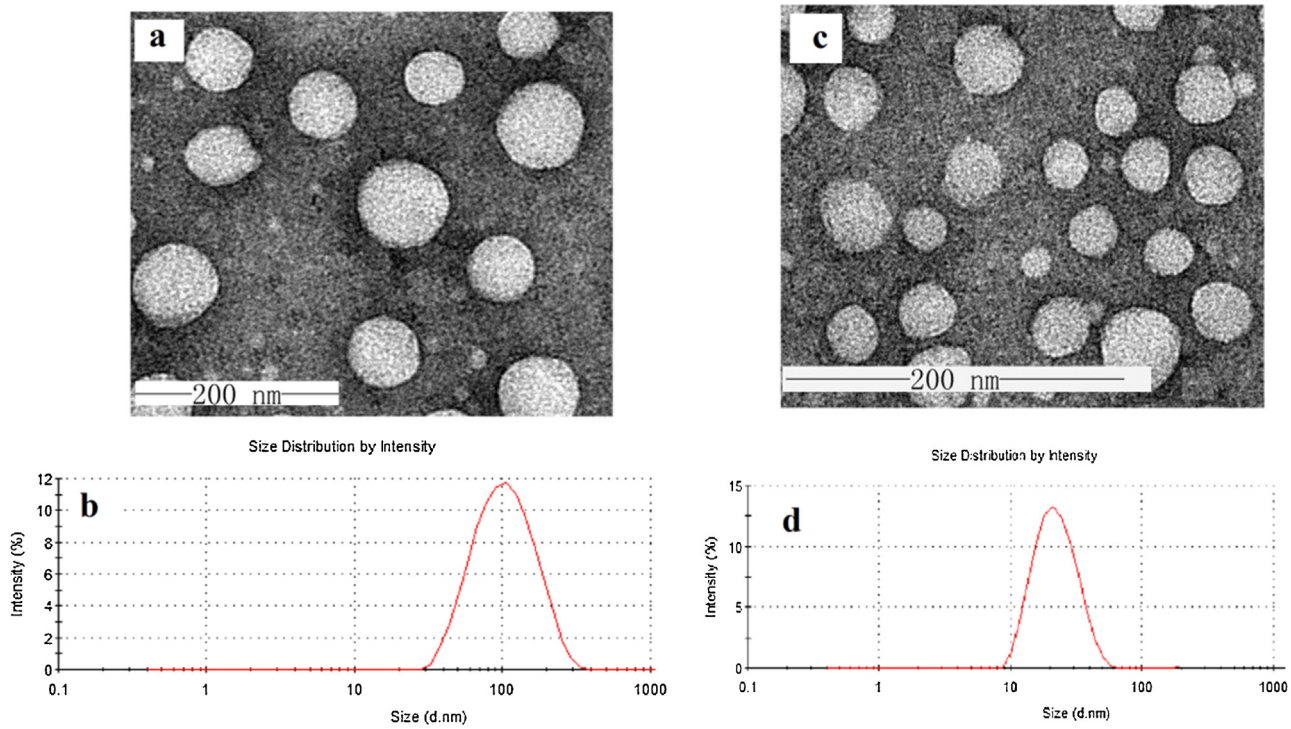

Fig. 4. TEM image of copolymer micelles at pH 7.4 (a) mPEG-b-PLA-b-DNP-PHis; (c) mPEG-b-PLA-b-PHis; particle size and distribution of copolymer micelles determined by DLS at pH 7.4; (b) mPEG-b-PLA-b-DNP-PHis; (d) mPEG-b-PLA-b-PHis). The data of mPEG-b-PLA-b-PHis copolymer that have been published before were used again for comparision [24].

acceleration voltage of 100 KV. Each sample was placed on a carbon-coated copper grid, negatively stained with 2% phosphotungstic acid aqueous solution followed by air-drying at room temperature.

2.9. In vitro *release of drug-loaded micelles*

In vitro release of DOX loaded micelles was studied using a dialysis bag (MWCO 12,000 Da) under sink conditions. Briefly, a series of 2.0 mL of DOX-loaded micelle solutions were transferred in dialysis bags and immersed in conical flasks containing different PBS buffers (pH 7.4, pH 6.8, pH 6.0, pH 5.0, 50 mL). The conical flasks were put in a shaking bed (Incubator shaker KYC 100B, Shanghai FUMA TEST EQUIPMENT Co., Ltd.) with a shaking rate of 100 rpm at 37 °C. The medium was replaced with fresh buffer solution at pre-determined time intervals. The released DOX was determined by a fluorescence detector with excitation wavelength at 480 nm and emission wavelength at 550 nm [34].

2.10. *Confocal laser scanning microscope (CLSM)*

MCF-7 cells were seeded on a cover-slide system at the density of 4×10^5 cells/well in a humidifier with 5% CO_2 atmosphere for 24 h at 37 °C followed by incubation with the test formulations. After incubation for pre-determined time intervals, the cells were stained with 100 nM Lyso-Tracker Green, and incubated for 30 min, the culture medium was removed and the cells were rinsed with cold PBS, then fixed with 4% paraformaldehyde for 30 min. The cells were stained with 10 μg/mL Hoechst 33258 for 15 min. The

microscope images of cells were captured using a CLSM (Olympus FV1000-IX81, Japan).

2.11. Cellular uptake

MCF-7 cells were plated (1×10^6 cells/well) in 6-well plates and incubated overnight at 37 °C under 5% CO_2. (i) DOX solution (5 μg/mL) was added and incubated for 0.5, 1, 2, 4, 6, 8 h to study the time dependence of cellular uptake, (ii) DOX solution (5 μg/mL) was added and incubated for 3 h at both 4 °C and 37 °C to study the energy dependence of cellular uptake. To study the effect of different inhibitors on the cellular uptake of copolymer micelles, the cells were pre-incubated with following inhibitors at concentrations which were not toxic to the cells [35,36]. (i) 1 mg/mL sodium azide for 1 h, (ii) 10 μg/mL chlorpromazine for 30 min, (iii) 50 μM amiloride for 1 h, (iv) 50 μM β-cyclodextrin for 30 min. DOX solution was then added and incubated for an additional 3 h. After incubation, the cells were then washed 3 times with PBS, trypsinized, harvested, and resuspended in methanol/water (7:3) solvent. The mean fluorescence intensity of cellular uptake was measured at an excitation wavelength of 480 nm and an emission wavelength of 550 nm.

2.12. DiR fluorescence real-time tumor imaging

MCF-7 cells were injected to female BALB/c nude mice by subcutaneous injection of 1×10^7 cells suspending in saline solution. When the tumor reached approximately 150–200 mm^3, 0.2 mL of DiR-loaded mPEG-b-PLA-b-PHis and mPEG-b-PLA-b-DNP-PHis micelles were intravenously injected through tail vein, respectively. The time-dependent biodistribution of the two micelles in MCF-7 tumor-bearing nude mice was imaged by the Kodak *in vivo* imaging system FX PRO (Carestream Health, Inc., USA) at different time points post injection, respectively. The mice under anesthetic state via inhalation of Gerolan Sol were automatically moved into the imaging chamber for scanning. After 48 h, the mice were sacrificed and major organs and tumors were harvested. Each organ and tumor was rinsed with saline for three times followed by the capture of fluorescent images.

2.13. Statistical analysis

All experiments were performed at least three times. Quantitative data are presented as the mean ± S.D. Statistical comparisons were determined by the analysis of variance (VANOVA) among ≥3 groups or Student's *t*-test between 2 groups. *P*-values < 0.05 and *P*-values < 0.01 were considered statistically significant.

3. Results and discussion

3.1. Characterization of the copolymers

The typical ^{1}H NMR spectra of the mPEG-b-PLA-b-DNP-PHis and mPEG-b-PLA-b-PHis triblock copolymers are shown in Fig. 2.

All the chemical shifts were expressed in parts per million (δ) relative to the tetramethylsilane (TMS) signal. ^{1}H NMR spectrum (DMSO-d_6) of mPEG-b-PLA-b-DNP-PHis showed the characteristic peaks of poly (N^{im}-DNP-L-histidine) at δ 7.91–8.90 ppm (proton h on phenyl group, DNP), δ_i 4.90 ppm (—CH—), δ_f 1.28 ppm (—C(CH_3)$_2$—) as well as the characteristic peaks of mPEG-PLA at δ_c 5.14 ppm (—COCH(CH_3)O—), δ_a 3.51 ppm (—OCH_2CH_2O—), δ_b 3.25 ppm (—OCH_3), δ_d 1.45 ppm (—COCH(CH_3)O—), δ_e 4.28 ppm (—$COOCH_2CH_2$O—) and δ_f 1.28(—C(CH_3)$_2$—). The disappearance of the characteristic peaks at —7.91–8.90 ppm (protons on phenyl group, DNP) indicates that mPEG-b-PLA-b-PHis copolymer was obtained by cutting off the DNP groups (Fig. 2b). The characteristic results of different copolymers are shown in Table 1. All the copolymers showed unimodal distribution with a polydispersity less than 1.2.

Compared to the titration curve of mPEG-b-PLA-b-PHis, the mPEG-b-PLA-b-DNP-PHis copolymer showed similar buffering pH range from pH 7.4 to 4.0 (p$K\alpha \sim 6.25$) (Fig. 3A), but a slight decrease in the buffering capacity from 26.76% to 19.26% (Table 1). This was probably attributed to the shielding effect on unsaturated nitrogen caused by the steric hindrance of DNP groups in the PHis block [37]. In addition, the electron-withdrawing effect of DNP group might also reduce the electron cloud density around unsaturated nitrogen [38], leading to a decrease in the buffering capacity.

The CMC values of the two copolymers were measured by the change of fluorescence spectrum of pyrene due to its selective partition into hydrophobic micellar core in the copolymer solution [39]. As shown in Fig. 3B, the remarkable increase in the intensity ratio(I_{336}/I_{334}) of the pyrene indicates the copolymer self-assembled into micelles [30]. The CMC values of the copolymers estimated from the plots are shown in Table 1. The mPEG-b-PLA-b-DNP-PHis showed slightly lower CMC value than mPEG-b-PLA-b-PHis copolymer, indicating that the substitution of DNP group cause no significant change in the hydrophobicity of the copolymer.

3.2. Effect of DNP group on the physio-chemical properties of the PHis based micelles

3.2.1. The formulation characteristics of the micelles

To investigate the effect of DNP modification on the formulation characteristics of the micelles, the particle size and size distribution of the micelles were first measured. TEM images revealed that the self-assembly copolymer micelles were spherical in shape with diameters of around 100 nm (mPEG-b-PLA-b-DNP-PHis) or 30 nm (mPEG-b-PLA-b-PHis) (Fig. 4a and c). As shown in Fig. 4b and d, the mean diameter of mPEG-b-PLA-b-DNP-PHis and mPEG-b-PLA-b-PHis micelles determined by DLS was 112 nm and 28 nm with good polydispersity indexes, respectively. The micellar size determined by TEM correlated well with that measured by DLS. The mPEG-b-PLA-b-DNP-PHis copolymer micelles showed much bigger particle size than mPEG-b-PLA-b-PHis micelles, which was probably due to the formation of big hydrophobic core in the micelles arising from benzyl moiety of the DNP group. The characterization of DOX loaded copolymer micelles are shown in Table 2. The DNP modified copolymer micelles showed similar EE % and DL % with mPEG-b-PLA-b-PHis micelles.

3.2.2. pH induced micellar structure change and drug release

The change of the micellar inner core as a function of pH was investigated with pyrene as a probe. The fluorescence intensity ratios (I_{336}/I_{334}) of pyrene under different pH conditions are shown in Fig. 5. The mPEG-b-PLA-b-DNP-PHis micelles showed a gradual decrease in I_{336}/I_{334} value as the pH decreased from 8.5 to 6.5, suggesting pH-dependent polarity increase in the micellar core. The polarity increase was obviously attributed to the progressive protonation of PHis block of the copolymer with pH decrease [40].

DOX release profiles from the copolymer micelles under different pH conditions (pH 7.4, pH 6.8, pH 6.0 and pH 5.0) are shown in Fig. 5. Both copolymer micelles showed a pH accelerated DOX release trend as characterized by the relatively faster DOX release as the pH decreased from 7.4 to 5.0. Due to the relative high drug leakage at pH7.4 (around 30% at 2 h), the pH dependency of the DOX release rate remained to be improved. This leads to a requirement for chemical modification to the saturated nitrogen of the copolymer in order to reduce the drug leakage at neutral pH via enhancement of the stability of drug incorporated micelles. The

Table 2
characterization of DOX-loaded copolymer micelle system.

Drug	Copolymer	Particle size	Zeta potential	0 h		24 h	
				DL (%)	EE (%)	DL (%)	EE (%)
Doxorubicin	mPEG-b-PLA-b-PHis	36.9	−3.91	7.95	86.4	3.89	40.5
	mPEG-b-PLA-b-DNP-PHis	114.8	−3.77	7.79	84.5	4.08	42.5

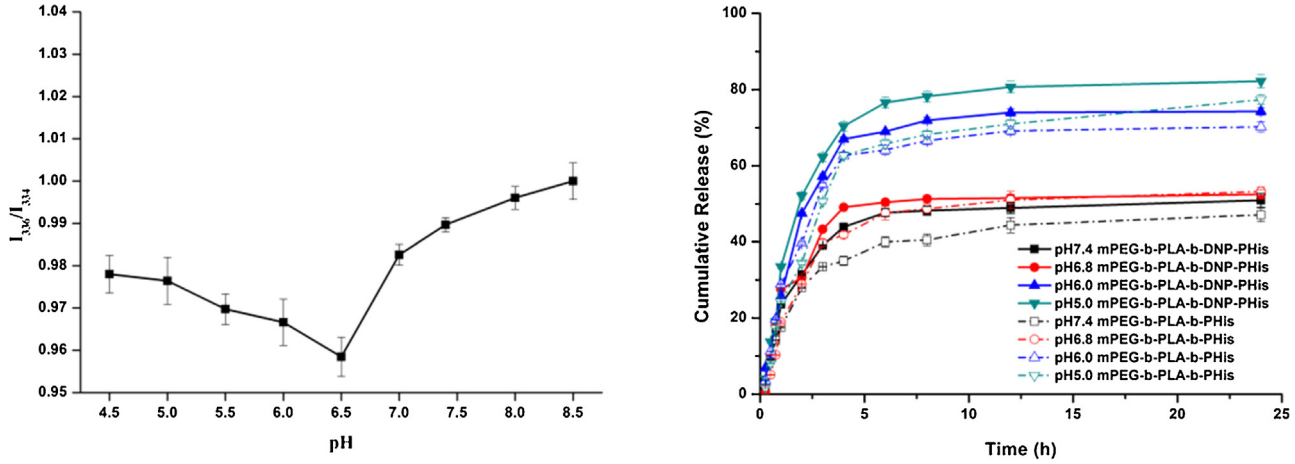

Fig. 5. The fluorescence intensity ratio of I_{336}/I_{334} as a function of pH in mPEG-b-PLA-b-DNP-PHis; *In vitro* drug release profiles from DOX/mPEG-b-PLA-b-DNP-PHis loaded micelles under different pH values (pH 7.4, 6.8, 6.0, 5.0). The data of mPEG-b-PLA-b-PHis copolymer that have been published before were used again for comparision [24].

triggering pH of mPEG-b-PLA-b-DNP-PHis micelles was around 6.0, which was close to the endo-lysosomal pH of the cells. These results indicate that the DNP modification to PHis showed no adverse effect on the pH responsive properties of the micelles.

3.3. Effect of DNP on the cytotoxicity, cellular uptake and endo-lysosomal escape

3.3.1. Cellular uptake of the micelles

The cellular uptake of the copolymer micelles by MCF-7 cells was determined by measuring the uptake of DOX in the cells. The mPEG-b-PLA-b-DNP-PHis micelles showed similar uptake efficiency with mPEG-b-PLA-b-PHis micelles until 4 h, but a significantly higher uptake efficiency afterwards ($p < 0.05$) (Fig. S1A). According to recent studies on the intracellular trafficking of nanoparticles, the cellular uptake of nanoparticles in cells depends on their physiochemical properties such as size, shape of particles and surface charge [41–43]. Since the two micelles had similar shape and surface change, the uptake difference was clearly attributed to their particle size. Particle size is a key property that affects the endocytic pathway and cellular uptake efficiency. Previous study demonstrated that larger particles have enough free energy to be wrapped by cell membrane and accumulate more efficiently in cells [42].

The cellular uptake of copolymer micelles was found to be an energy-dependent process as evidenced by the significant reduction (decreased about 30%) in the uptake of all the copolymer micelles at 4 °C [44]. To understand the uptake pathways of the two micelles, the intracellular trafficking of the micelles was studied using three different endocytosis inhibitors. Chlorpromazine, amiloride and β-cyclodextrin were used as inhibitor to evaluate clathrin, macropinocytosis and caveolae uptake pathway, respectively [45]. As shown in Fig. 6S1B, the uptake rate of the mPEG-b-PLA-b-PHis and mPEG-b-PLA-b-DNP-PHis copolymer micelles was inhibited to 73% and 63%, 90% and 86%, 89% and 78% by chlorpromazine, amiloride and β-cyclodextrin, respectively. These results indicate that clathrin-mediated endocytosis was a primary uptake pathway for the two PHis based compolymer micelles. However, The higher cellular uptake inhibition by the inhibitors may indicate higher cellular uptake efficiency of mPEG-b-PLA-b-DNP-PHis copolymer micelles than mPEG-b-PLA-b-PHis micelles.

3.3.2. Copolymers facilitated endo-lysosomal escape of DOX

The intracellular localization of DOX from the micelles (mPEG-b-PLA-b-DNP-PHis and mPEG-b-PLA-b-PHis micelles) was investigated using confocal scanning microscopy on MCF-7 cells with mPEG-b-PLA micelles and free DOX as control. The CLSM photos of the micelles incubated with MCF-7 cells for different time intervals are presented in Fig.S2. The cell nuclei and endo-lysosome were labeled with Hoechst 33258 (blue) and LysoTracker DND-26 (green), respectively. The mPEG-b-PLA-b-DNP-PHis and mPEG-b-PLA-b-PHis copolymer showed yellow fluorescence (the overlap of DOX with lysotracker) at 15 min and a strong purple fluorescence (the overlap of DOX with nuclei staining Hoechst) at 6 h, indicating the initial encapsulation in primary endosome and the escape of the DOX from endosome into nuclei afterwards. As noted from Fig. S2, the mPEG-b-PLA-b-DNP-PHis showed a slightly less intensity of red fluorescence in nuclei than mPEG-b-PLA-b-PHis, indicating less efficiency in facilitating endosomal escape of DOX. This was probably attributed to the lower buffering capacity of the mPEG-b-PLA-b-DNP-PHis copolymers. As compared to the PHis based micelles, the mPEG-PLA micelles showed much weaker purple fluorescence after incubation for 4 h due to the incapability of the copolymer in facilitation of DOX endosomal escape.

3.3.3. pH-dependent cytotoxicity

The *in vitro* cytotoxicity of copolymer micelles was evaluated in MCF-7 cells using MTT assays with DOX solution as controls. As shown in Fig. 6, the blank micelles of the copolymers showed no cytotoxicity against MCF-7 cells after 48 h incubation [46]. In comparison to DOX solution, which showed remarkable cytotoxicity under all pH conditions, the DOX-loaded micelles revealed slightly lower cytotoxicity under neutral pH (pH 7.4), suggesting that the DOX release from micelles followed a sustained release

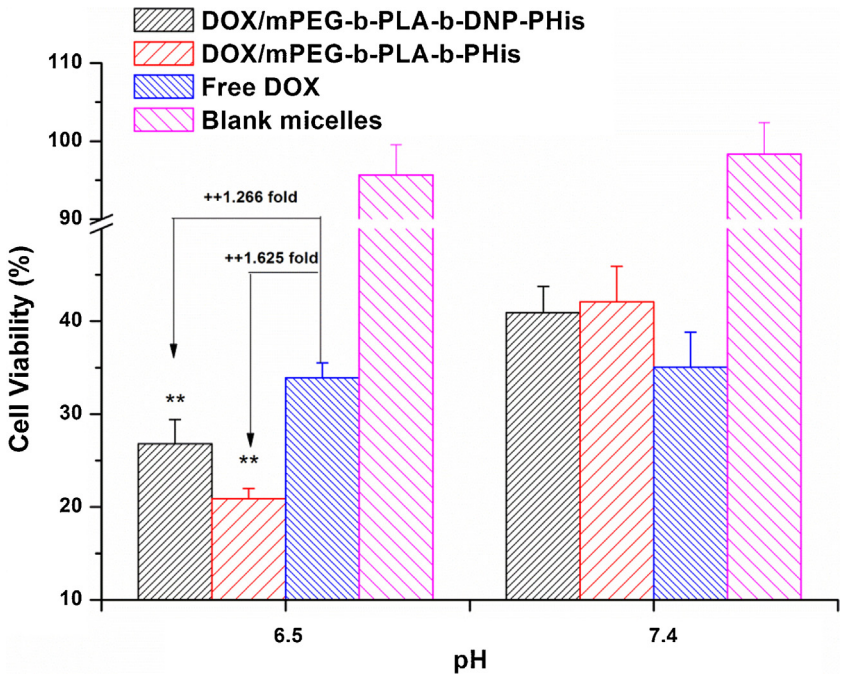

Fig. 6. The cytotoxicity of DOX-loaded micelles and DOX solution at different pH_s against MCF-7 cells ($n = 3$). All data are present as mean ± SD. $^{**}P < 0.01$, significantly different from the micelles under neutral pH (pH 7.4), $^{++}P < 0.01$: significantly different from the free DOX. The data of mPEG-b-PLA-b-PHis copolymer that have been published before were used again for comparision [24].

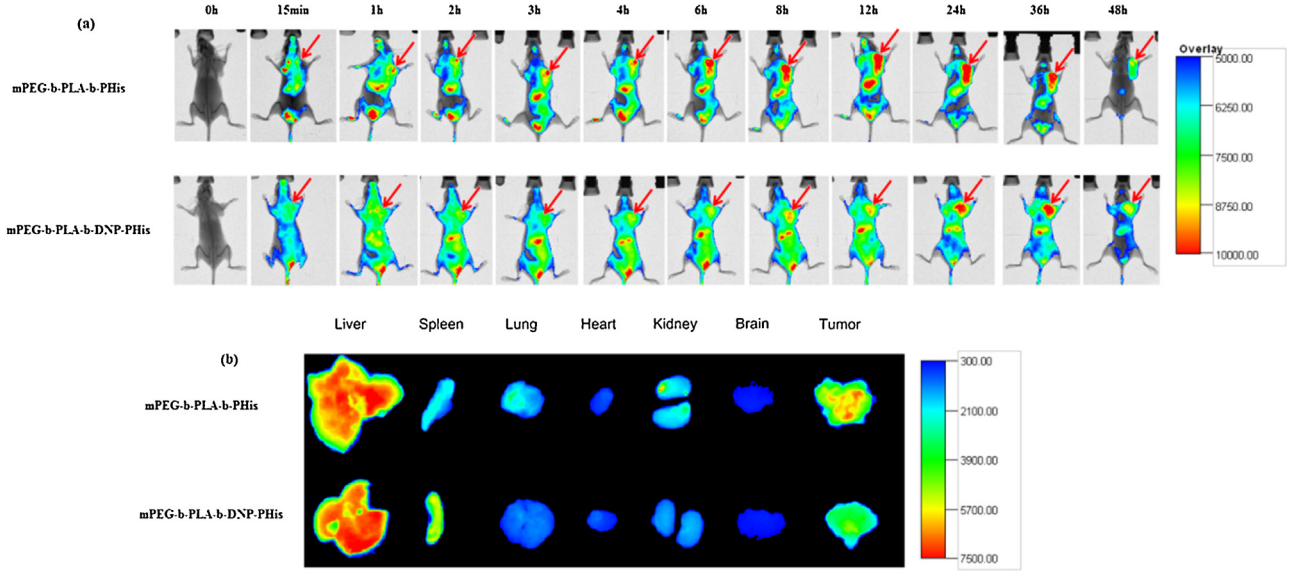

Fig. 7. The *in vivo* non-invasive images of time-dependent whole body imaging of MCF-7 tumor-bearing mice after i.v. injection of mPEG-b-PLA-b-PHis and mPEG-b-PLA-b-DNP-PHis (a). The *ex vivo* optical images of tumors and organs of MCF-7 tumor-bearing mice sacrificed at 48 h after i.v. injection of mPEG-b-PLA-b-PHis and mPEG-b-PLA-b-DNP-PHis (b).

pattern [47]. However, the cytotoxicity of DOX loaded micelles was significantly increased at acidic pH 6.5 compared to that at neutral pH due to the accelerated DOX release under acidic environment (The cell viability data at pH 6.0 are not shown in Fig. 6 due to the acidic pH has a negative effect on the growth of the cells).

Moreover, the increased cytotoxicity at pH 6.5 may be due to the combined effect of increased protonation of imidazole in PHis group on the micelles surface at tumor pH, which increases binding to the cell membrane, leading to great internalization and, thus, greater micelles cytotoxicity [48]. DOX/mPEG-b-PLA-b-DNP-PHis showed slightly lower cytotoxicity against MCF-7 cells than DOX/mPEG-b-PLA-b-PHis micelles at pH 6.5. Considering the fact that DOX/mPEG-b-PLA-b-DNP-PHis micelles were endocytosed more efficiently into the MCF-7 cells than DOX/mPEG-b-PLA-b-PHis micelles, the relatively lower cytotoxicity against the cells could be attributed to the lower buffering capacity of the copolymers, leading to more DOX sequestrated in the endo-lysosome. These findings suggest that DNP modification to the saturated nitrogen of PHis block still remains endo-lysosomal pH triggered drug release and PHis facilitated endo-lysosomal escape properties.

3.3.4. In vivo *biodistribution of copolymer micelles.*

The effect of DNP modification on the *in vivo* biodistribution of the copolymer based micelles was assessed via non-invasive near-

infrared fluorescence (NIRF) image with DiR as a probe [49]. DiR is a lipophilic dialkylcarbocyanine dye that fluoresces in the NIR band, which prevents any light absorption by tissues, auto-fluorescence and scattering usually associated with the use of visible light dyes [50]. The loading efficiency of DiR for mPEG-b-PLA-b-DNP-PHis micelles and mPEG-b-PLA-b-PHis micelles were 93.2% and 91.5%, respectively. As shown in Fig. 7a, the mPEG-b-PLA-b-DNP-PHis micelles showed apparent accumulation in tumor until 4 h as characterized by the observable DiR fluorescences in tumor. As compared to mPEG-b-PLA-b-DNP-PHis micelles, the mPEG-b-PLA-b-PHis micelles showed much faster accumulation of DiR in tumor within 1 h. The major organs (heart, liver, spleen, lung, kidney and brain) and tumor tissues were isolated and the *ex vivo* images were further studied (Fig. 7b). The mPEG-b-PLA-b-DNP-PHis micelles showed less stronger fluorescence intensity in tumor tissue than mPEG-b-PLA-b-PHis micelles, indicating a worse tumor targeting. Moreover, the mPEG-b-PLA-b-DNP-PHis revealed stronger fluorescence intensity in liver and spleen than mPEG-b-PLA-b-PHis micelles [51].

The different biodistribution profiles of the two micelles were obviously attributed to the particle size difference caused by the DNP modification. The particle size of the nanoparticles has been considered as a key factor to affect the pharmacokinetic and biodistribution of them [52,53]. A previous study also confirmed that 20 nm peglylated nanoparticles accumulated in the tumor tissue more rapidly than 100 nm nanoparticles due to the higher extravasation rate of smaller peglylated nanoparticles from the leaky vasculature into the tumor tissues. Moreover, the size of nanoparticles has a substantial effect on the protein absorption on the surface of particles. Protein absorption on small nanoparticles was much less than the same nanoparticles with a large size [54]. The mechanism of hepatic and spleen uptake was mediated by the surface absorption of proteins and the subsequent opsonization. *In vitro* studies showed that the surface protein absorption led to an increase in the uptake of nanoparticles by kupffer cells [55]. The lower surface absorption of protein to smaller nanoparticles was probably caused by the higher surface PEG density than larger nanoparticle. This explains the higher accumulation of mPEG-b-PLA-b-DNP-PHis micelles in the liver and spleen than mPEG-b-PLA-b-PHis micelles.

4. Conclusions

In this study, a series of PHis based copolymers were synthesized to investigate the effect of DNP substitution of PHis block on the physio-chemical and biodistribution properties of the micelles. The DNP substitution to the saturation nitrogen of the PHis showed little effect on the attractive feature of PHis based micelles, *i.e.* pH triggered drug release and PHis facilitated endosomal escape, indicating that the saturated nitrogen can serve as a valuable chemical modification site to improve the quality of the micelles or to impart a new function. However, the DNP substitution significantly increased the particle size of the copolymer micelles, leading to the moderately compromised *in vivo* tumor targeting. Therefore, careful selection of the substitution group is necessary for a successful chemical modification.

Conflict of interest

The authors declare no competing financial interest.

Acknowledgments

The authors are grateful to the financial support from the National Natural Science Foundation of China (81273448) as well as the program for Liaoning Excellent Talents in university (LR 2014029), Career Development Support Plan for Young and Middle-aged Teachers in Shenyang Pharmaceutical University.

Appendix A. Supplementary data

Supplementary data associated with this article can be found, in the online version, at http://dx.doi.org/10.1016/j.colsurfb.2015.12.032.

References

[1] E.S. Lee, K.T. Oh, D. Kim, Y.S. Youn, Y.H. Bae, Tumor pH-responsive flower-like micelles of poly(L-lactic acid)-b-poly(ethylene glycol)-b-poly(L-histidine), J. Control. Release 123 (2007) 19–26.
[2] K. Seo, D. Kim, pH-dependent hemolysis of biocompatible imidazole-grafted polyaspartamide derivatives, Acta Biomater. 6 (2010) 2157–2164.
[3] E.S. Lee, K. Na, Y.H. Bae, Super pH-sensitive multifunctional polymeric micelle, Nano Lett. 5 (2005) 325–329.
[4] H. Wu, L. Zhu, V.P. Torchilin, pH-sensitive poly(histidine)-PEG/DSPE-PEG co-polymer micelles for cytosolic drug delivery, Biomaterials 34 (2013) 1213–1222.
[5] H.A. Hirsch, D. Iliopoulos, P.N. Tsichlis, K. Struhl, Metformin selectively targets cancer stem cells, and acts together with chemotherapy to block tumor growth and prolong remission, Cancer Res. 69 (2009) 7507–7511.
[6] J.S. Park, T.H. Han, K.Y. Lee, S.S. Han, J.J. Hwang, D.H. Moon, S.Y. Kim, Y.W. Cho, *N*-acetyl histidine-conjugated glycol chitosan self-assembled nanoparticles for intracytoplasmic delivery of drugs: endocytosis, exocytosis and drug release, J. Control. Release 115 (2006) 37–45.
[7] K.T. Oh, H. Yin, E.S. Lee, Y.H. Bae, Polymeric nanovehicles for anticancer drugs with triggering release mechanisms, J. Mater. Chem. 17 (2007) 3987–4001.
[8] E.S. Lee, Z. Gao, Y.H. Bae, Recent progress in tumor pH targeting nanotechnology, J. Control. Release 132 (2008) 164–170.
[9] G.H. Gao, Y. Li, D.S. Lee, Environmental pH-sensitive polymeric micelles for cancer diagnosis and targeted therapy, J. Control. Release 169 (2013) 180–184.
[10] Y.H. Bae, H. Yin, Stability issues of polymeric micelles, J. Control. Release 131 (2008) 2–4.
[11] H. Yin, E.S. Lee, D. Kim, K.H. Lee, K.T. Oh, Y.H. Bae, Physicochemical characteristics of pH-sensitive poly(L-Histidine)-b-poly(ethylene glycol)/poly(L-lactide)-b-poly(ethylene glycol) mixed micelles, J. Control. Release 126 (2008) 130–138.
[12] E.S. Lee, K. Na, Y.H. Bae, Polymeric micelle for tumor pH and folate-mediated targeting, J. Control. Release 91 (2003) 103–113.
[13] E.S. Lee, K. Na, Y.H. Bae, Doxorubicin loaded pH-sensitive polymeric micelles for reversal of resistant MCF-7 tumor, J. Control. Release 103 (2005) 405–418.
[14] G.M. Kim, Y.H. Bae, W.H. Jo, pH-induced micelle formation of poly(histidine-co-phenylalanine)-block-poly(ethylene glycol) in aqueous media, Macromol. Biosci. 5 (2005) 1118–1124.
[15] D. Kim, E.S. Lee, K.T. Oh, Z.Q. Gao, Y.H. Bae, Doxorubicin-loaded polymeric micelle overcomes multidrug resistance of cancer by double-targeting folate receptor and early endosomal pH, Small 4 (2008) 2043–2050.
[16] G.J.M. Habraken, K.H.R.M. Wilsens, C.E. Koning, A. Heise, Optimization of *N*-carboxyanhydride (NCA) polymerization by variation of reaction temperature and pressure, Polym. Chem. 2 (2011) 1322–1330.
[17] H.R. Kricheldorf, Polypeptides and 100 years of chemistry of alpha-amino acid *N*-carboxyanhydrides, Angew. Chem. Int. Ed. Engl. 45 (2006) 5752–5784.
[18] D. Mavrogiorgis, P. Bilalis, A. Karatzas, D. Skoulas, G. Fotinogiannopoulou, H. Iatrou, Controlled polymerization of histidine and synthesis of well-defined stimuli responsive polymers. Elucidation of the structure-aggregation relationship of this highly multifunctional material, Polym. Chem. 5 (2014) 6256–6278.
[19] M. Fridkin, S. Shaltiel, A new route to polyamino acids containing histidine, Arch. Biochem. Biophys. 147 (1971) 767–771.
[20] S.Y. Li, R. Sun, H.X. Wang, S. Shen, Y. Liu, X.J. Du, Y.H. Zhu, W. Zhu, Combination therapy with epigenetic-targeted and chemotherapeutic drugs delivered by nanoparticles to enhance the chemotherapy response and overcome resistance by breast cancer stem cells, J. Control. Release 205 (2015) 7–14.
[21] Sangeetha Krishnamurthy, Xiyu Ke, Y.Y. Yang, Delivery of therapeutics using nanocarriers for targeting cancer cells and cancer stem cells, Nanomed.: Nanotechnol. Biol. Med. 10 (2015) 143–160.
[22] H.K. de Wolf, C.J. Snel, F.J. Verbaan, R.M. Schiffelers, W.E. Hennink, G. Storm, Effect of cationic carriers on the pharmacokinetics and tumor localization of nucleic acids after intravenous administration, Int. J. Pharm. 331 (2007) 167–175.
[23] R. Liu, B. He, D. Li, Y. Lai, J.Z. Tang, Z. Gu, Synthesis and characterization of poly(ethylene glycol)-b-poly(L-histidine)-b-poly(L-lactide) with pH-sensitivity, Polymer 53 (2012) 1473–1482.
[24] X. Zhang, D. Chen, S. Ba, J. Zhu, J. Zhang, W. Hong, X. Zhao, H. Hu, M. Qiao, Poly(L-histidine) based triblock copolymers: pH Induced reassembly of copolymer micelles and mechanism underlying endolysosomal escape for intracellular delivery, Biomacromolecules 15 (2014) 4032–4045.

[25] M. Ou, R. Xu, S.H. Kim, D.A. Bull, S.W. Kim, A family of bioreducible poly(disulfide amine)s for gene delivery, Biomaterials 30 (2009) 5804–5814.
[26] Z. Zhong, J. Feijen, Low molecular weight linear polyethylenimine-b-poly(ethylene glycol)-b-polyethylenimine triblock copolymers synthesis,characterization, and in vitro gene transfer properties, Biomacromolecules 6 (2005) 3440–3448.
[27] W. Park, D. Kim, H.C. Kang, Y.H. Bae, K. Na, Multi-arm histidine copolymer for controlled release of insulin from poly(lactide-co-glycolide) microsphere, Biomaterials 33 (2012) 8848–8857.
[28] M. Cai, K. Zhu, Y. Qiu, X. Liu, Y. Chen, X. Luo, pH and redox-responsive mixed micelles for enhanced intracellular drug release, Colloids Surf. B 116 (2014) 424–431.
[29] A. Cunningham, N.R. Ko, J.K. Oh, Synthesis and reduction-responsive disassembly of PLA-based mono-cleavable micelles, Colloids Surf. B 122 (2014) 693–700.
[30] C.Y. Zhang, Y.Q. Yang, T.X. Huang, B. Zhao, X.D. Guo, J.F. Wang, L.J. Zhang, Self-assembled pH-responsive MPEG-b-(PLA-co-PAE) block copolymer micelles for anticancer drug delivery, Biomaterials 33 (2012) 6273–6283.
[31] L.Y. Qiu, Y.H. Bae, Self-assembled polyethylenimine-graft-poly(ε-caprolactone) micelles as potential dual carriers of genes and anticancer drugs, Biomaterials 28 (2007) 4132–4142.
[32] S.C. Kim, D.W. Kim, Y.H. Shim, J.S. Bang, H.S. Oh, S.W. Kim, M.H. Seo, In vivo evaluation of polymeric micellar paclitaxel formulation:toxicity and efficacy, J. Control. Release 72 (2001) 191–202.
[33] S. Li, Q. He, T. Chen, W. Wu, K. Lang, Z.M. Li, J. Li, Controlled co-delivery nanocarriers based on mixed micelles formed from cyclodextrin-conjugated and cross-linked copolymers, Colloids Surf. B 123 (2014) 486–492.
[34] H. Yin, Y.H. Bae, Physicochemical aspects of doxorubicin-loaded pH-sensitive polymeric micelle formulations from a mixture of poly(L-histidine)-b-poly(ethylene glycol)/poly(L-lactide)-b-poly(ethylene glycol), Eur. J. Pharm. Biopharm. 71 (2009) 223–230.
[35] O.P. Perumal, R. Inapagolla, S. Kannan, R.M. Kannan, The effect of surface functionality on cellular trafficking of dendrimers, Biomaterials 29 (2008) 3469–3476.
[36] S.M. Alex, C.P. Sharma, Enhanced intracellular uptake and endocytic pathway selection mediated by hemocompatible ornithine grafted chitosan polycation for gene delivery, Colloids Surf. B 122 (2014) 792–800.
[37] N.H. Martin, N.W. Allen III, K.D. Moore, L. Vo, A proton NMR shielding model for the face of a benzene ring, J. Mol. Struct.: THEOCHEM 454 (1998) 161–166.
[38] H. Kuroda, S. Nakatsuchi, N. Kitao, T. Nakagawa, Radical polymerization of methacrylates having acetylenic moiety activated by electron-withdrawing group as a reactive functional group, React. Funct. Polym. 66 (2006) 229–238.
[39] K. Na, K.H. Lee, pH-sensitivity and pH-dependent interior structural change of self-assembled hydrogel nanoparticles of pullulan acetate/oligo-sulfonamide conjugate, J. Control. Release 97 (2004) 513–525.
[40] E.S. Lee, H.J. Shin, K. Na, Y.H. Bae, Poly(L-histidine)—PEG block copolymer micelles and pH-induced destabilization, J. Control. Release 90 (2003) 363–374.
[41] G. Sharma, D.T. Valenta, Y. Altman, S. Harvey, H. Xie, S. Mitragotri, J.W. Smith, Polymer particle shape independently influences binding and internalization by macrophages, J. Control. Release 147 (2010) 408–412.
[42] C.L. Lo, M.H. Chou, P.L. Lu, I.W. Lo, Y.T. Chiang, S.Y. Hung, C.Y. Yang, S.Y. Lin, S.P. Wey, J.M. Lo, G.H. Hsiue, The effect of PEG-5K grafting level and particle size on tumor accumulation and cellular uptake, Int. J. Pharm. 456 (2013) 424–431.
[43] L. Bekale, D. Agudelo, H.A. Tajmir-Riahi, The role of polymer size and hydrophobic end-group in PEG-protein interaction, Colloids Surf. B 130 (2015) 141–148.
[44] K. Xiao, Y. Li, J. Luo, J.S. Lee, W. Xiao, A.M. Gonik, R.G. Agarwal, K.S. Lam, The effect of surface charge on *in vivo* biodistribution of PEG-oligocholic acid based micellar nanoparticles, Biomaterials 32 (2011) 3435–3446.
[45] W. Xu, L. Cao, L. Chen, J. Li, X.F. Zhang, H.H. Qian, X.Y. Kang, Y. Zhang, J. Liao, L.H. Shi, Y.F. Yang, M.C. Wu, Z.F. Yin, Isolation of circulating tumor cells in patients with hepatocellular carcinoma using a novel cell separation strategy, Clin. Cancer Res. 17 (2011) 3783–3793.
[46] Y. Wu, W. Chen, F. Meng, Z. Wang, R. Cheng, C. Deng, H. Liu, Z. Zhong, Core-crosslinked pH-sensitive degradable micelles: a promising approach to resolve the extracellular stability *versus* intracellular drug release dilemma, J. Control. Release 164 (2012) 338–345.
[47] S.R. Yang, H.J. Lee, J.-D. Kim, Histidine-conjugated poly(amino acid) derivatives for the novel endosomolytic delivery carrier of doxorubicin, J. Control. Release 114 (2006) 60–68.
[48] D.R. Nogueira, L. Tavano, M. Mitjans, L. Perez, M.R. Infante, M.P. Vinardell, In vitro antitumor activity of methotrexate via pH-sensitive chitosan nanoparticles, Biomaterials 34 (2013) 2758–2772.
[49] Y. Sun, B. Yu, G. Wang, Y. Wu, X. Zhang, Y. Chen, S. Tang, Y. Yuan, R.J. Lee, L. Teng, S. Xu, Enhanced antitumor efficacy of vitamin E TPGS-emulsified PLGA nanoparticles for delivery of paclitaxel, Colloids Surf. B 123 (2014) 716–723.
[50] S. Luo, E. Zhang, Y. Su, T. Cheng, C. Shi, A review of NIR dyes in cancer targeting and imaging, Biomaterials 32 (2011) 7127–7138.
[51] Y. Zhang, H.F. Chan, K.W. Leong, Advanced materials and processing for drug delivery: the past and the future, Adv. Drug Deliv. Rev. 65 (2013) 104–120.
[52] R. Gref, Y. Minamitake, M.T. Peracchia, V. Trubetskoy, V. Torchilin, R. Langer, Biodegradable long-circulating polymeric nanospheres, Science 263 (1994) 1600–1603.
[53] H. Meng, M. Xue, T. Xia, Z. Ji, D.Y. Tarn, J.I. Zink, A.E. Nel, Use of size and a copolymer design feature to improve the biodistribution and the enhanced permeability and retention effect of doxorubicin loaded mesoporo us silica nanopar ticles in a murine xenog raft tumor model, ACS Nano 5 (2011) 4131–4144.
[54] S.D. Perrault, C. Walkey, T. Jennings, H.C. Fischer, W.C.W. Chan, Mediating tumor targeting efficiency of nanoparticles through design, Nano Lett. 9 (2009) 1909–1915.
[55] H.J. Yao, Y.G. Zhang, L. Sun, Y. Liu, The effect of hyaluronic acid functionalized carbon nanotubes loaded with salinomycin on gastric cancer stem cells, Biomaterials 35 (2014) 9208–9223.